Turbulence in globally coupled maps

M. G. Cosenza* and A. Parravano
Centro de Astrofísica Teórica, Facultad de Ciencias, Universidad de Los Andes, A. Postal 26 La Hechicera, Mérida 5251, Venezuela
(Received 15 November 1995)

The phenomenon of turbulence is investigated in the context of globally coupled maps. The local dynamics is given by the Chaté-Manneville minimal map previously used in studies of spatiotemporal intermittency in locally coupled map lattices. New features arise in the globally coupled system; for instance, the transition to turbulence takes place discontinuously at some critical values of the parameters of the system. The critical boundaries between different regimes (laminar, turbulent, and fully turbulent) of the system are calculated on the parameter space. Windows of turbulence are present in some ranges of the coupling parameter. The system also exhibits nontrivial collective behavior. A map for the instantaneous fraction of turbulent elements is proposed. This map describes many of the observed properties of the system. [S1063-651X(96)00106-7]

PACS number(s): 47.27.−i, 05.45.+b, 02.50.−r

I. INTRODUCTION

The transition to turbulence in confined systems and its relation to the routes to chaos has been a subject of much interest [1]. A very general scenario for the occurrence of turbulence is spatiotemporal intermittency, i.e., a sustained regime characterized by the coexistence of coherent-laminar and disordered-chaotic domains in space and time [2,3]. There are numerous studies of this phenomenon, some of the most extensive of which have been on model dynamical systems such as coupled map lattices (CML) [2,4–8]. The idea is that the ingredients of a CML — a discrete space, discrete time system of interacting elements whose states vary continuously according to specific functions — are sufficient to capture much of the phenomenology observed in complex spatiotemporal processes, in particular some relevant features of spatiotemporal intermittency and turbulence. In this respect, a CML can be viewed as a simplifying replacement for partial differential equations of hydrodynamics [9]. The onset of turbulence via spatiotemporal intermittency has mainly been investigated on CMLs with local, diffusive-type interactions on both low-dimensional Euclidean arrays [4–7] and on fractal lattices [8]. These studies have permitted the characterization of the transition to turbulence as a critical phenomenon in one and two dimensions and on several fractal dimensions with diverse local connectivities.

Recently, globally coupled elements have been a focus of attention in physics and biology [10–14], including systems such as Josephson junction arrays, charge density waves, multimode lasers, neural dynamics, ecological, and evolution models. Globally coupled maps [15] constitute a useful approach to the study of many processes on this kind of systems. Globally coupled maps can be regarded as an extension of a CML with diffusive coupling to infinite dimension, or as a limiting case of a system with long range interactions. Spatial concepts lose meaning and only temporal properties become relevant in globally coupled maps. These characteristics allow for simpler, mean-field descriptions of the behavior of the system.

*Electronic address: mcosenza@ula.ve

In this paper, we investigate the phenomenon of turbulence in the context of globally coupled maps. The local dynamics we employ is the elementary map of Chaté and Manneville [4], which has been shown to exhibit several properties of the transition to turbulence via spatiotemporal intermittency on locally coupled map lattices [4,8]. Our system of globally coupled Chaté and Manneville maps provides a situation to compare the roles that local and global interactions play on the occurrence of turbulence. Some different features arise in this model; for instance, the onset of turbulence appears to take place *discontinuously* at critical values of the parameters of the system. The model is presented and its statistical properties are numerically explored on its parameter space in Sec. II. In Sec. III, a map for the instantaneous fraction of turbulent elements in the system is proposed. This map model describes much of the behavior observed in Sec. II. The results are discussed in Sec. IV.

II. GLOBALLY COUPLED MINIMAL MAPS FOR TURBULENCE

We consider the globally coupled map system

$$x_{t+1}(i)=(1-\epsilon)f(x_t(i))+\frac{\epsilon}{N}\sum_{j=1}^{N} f(x_t(j)), \qquad (1)$$

where $x_t(i)$ gives the state of the lattice element i $(i=1,\ldots,,N=$ system size) at a discrete time step t, ϵ is the coupling parameter, and f is a map describing the local dynamics. The instantaneous mean field of the system is defined as

$$h_t=\frac{1}{N}\sum_{j=1}^{N} f(x_t(j)). \qquad (2)$$

While the choice of the local map f in Eq. (1) determines the details of the transition to turbulence, it need only possess a few general properties to observe spatiotemporal intermittency. The map introduced by Chaté and Manneville [4] contains such minimal requirements,

$$f(x)=\begin{cases}\dfrac{r}{2}(1-|1-2x|), & \text{if } x\in[0,1]\\ x, & \text{if } x>1,\end{cases} \tag{3}$$

with $r>2$. This map is chaotic as long as $f(x)$ remains in the interval $[0,1]$; however, when $f(x)>1$ the dynamics reaches a fixed point in one iteration. The local variable can thus be seen as a continuum of stable ''laminar'' fixed points $(x>1)$ adjacent to a chaotic repeller or ''turbulent'' phase $(x\in[0,1])$. For a coupled system the laminar phase is metastable, since sites in this state are stable to infinitesimal perturbations but possibly unstable to finite disturbances induced by the coupling.

In diffusively coupled map lattices, for a large enough coupling, the turbulent phase can propagate through the lattice in time producing sustained states of spatiotemporal intermittency [4,8]. Here, we investigate the corresponding phenomenon in the context of globally coupled maps [Eq. (1)] using the local map f [Eq. (3)]. This situation may be considered as spatiotemporal intermittency occurring on a diffusively coupled system in a spatially high-dimensional lattice, or as spatiotemporal intermittency in a limiting case of long range interactions. Thus the notions of spatial patterns and correlations characteristic of spatiotemporal intermittency in CMLs with local connections are lost and only temporal properties of the system become relevant. Above some threshold in parameter space (r,ϵ), and starting from random initial conditions, the globally coupled map system relaxes to a statistically stationary chaotic regime where each element displays intermittency between laminar and turbulent phases. As on locally coupled map lattices, the transition to this extended chaotic state can be monitored by the mean fraction of turbulent sites $\langle F\rangle$, a quantity that acts as the order parameter for the system [4]. We have calculated $\langle F\rangle$ as a function of the coupling parameter ϵ for several fixed values of r from a time average of the instantaneous turbulent fraction F_t, as

$$\langle F\rangle=\frac{1}{\tau}\sum_{t=1}^{\tau}F_t. \tag{4}$$

Typically 10^4 iterations were discarded before taking the time average in Eq. (4) and τ was fixed at the value 10^4. The typical system size used in the calculations was $N=10^4$. We have found that increasing the lattice sizes does not appreciably affect the results presented in this paper. The characteristics of the system also persist for small lattice sizes (up to $N=100$). As initial conditions, we use random cell values equally distributed between the turbulent and the laminar ranges. It is to be noticed that a minimum number of initially turbulent cells is always required to reach a sustained state of turbulence.

Figures 1(a) and 1(b) present plots of $\langle F\rangle$ versus ϵ for two different fixed values of r. For small coupling, the system reaches a uniformly laminar state. The onset of turbulence takes place discontinuously at a critical value of the coupling parameter, ϵ_c. The mean turbulent fraction $\langle F\rangle$ vanishes at a larger value of the coupling, giving rise to a relaminarization of the system; i.e., a second transition from turbulence to a uniform laminar state takes place at a value $\epsilon_c'>\epsilon_c$, establishing a well defined window of turbulence on the range $[\epsilon_c,\epsilon_c']$. Figure 1(b) shows that more than one of such windows of turbulence, separated by laminar gaps, can occur in globally coupled maps as the coupling is varied.

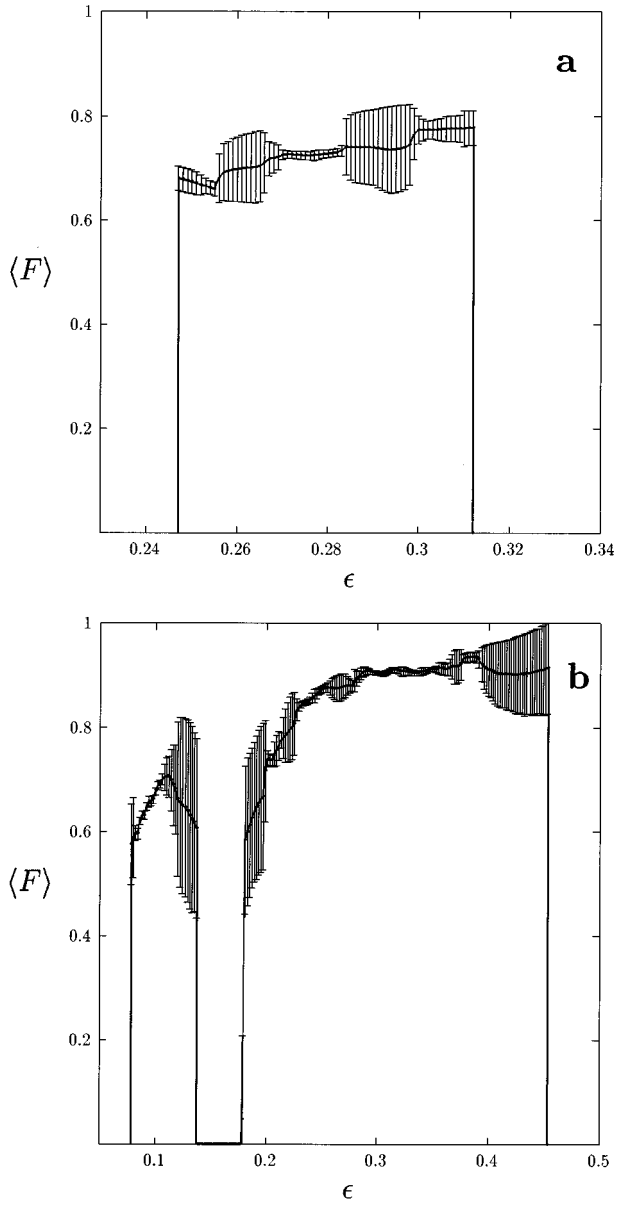

FIG. 1. Mean turbulent fraction $\langle F\rangle$ as a function of the coupling parameter ϵ. The local parameter is fixed at (a) $r=3$; (b) $r=2.6$. The error bars indicate ± 1 standard deviations.

Windows of spatiotemporal intermittency on a range of the coupling parameter have also been observed in coupled maps on fractal lattices with large enough connectivities [8]. In general, for CMLs with local interactions, the transition from a laminar regime to spatiotemporal intermittency (and vice versa, in the case of windows of turbulence) behaves in many aspects as a second order phase transition, characterized by the scaling relation $\langle F\rangle\sim(\epsilon-\epsilon_c)^{\beta}$, where β is a critical exponent [4,5,8]. In contrast, the transition between laminar states and turbulence in globally coupled maps appears as a discontinuous jump in the quantity $\langle F\rangle$, a feature associated to first order phase transitions. The absence of spatial relations in globally coupled maps rules out the pos-

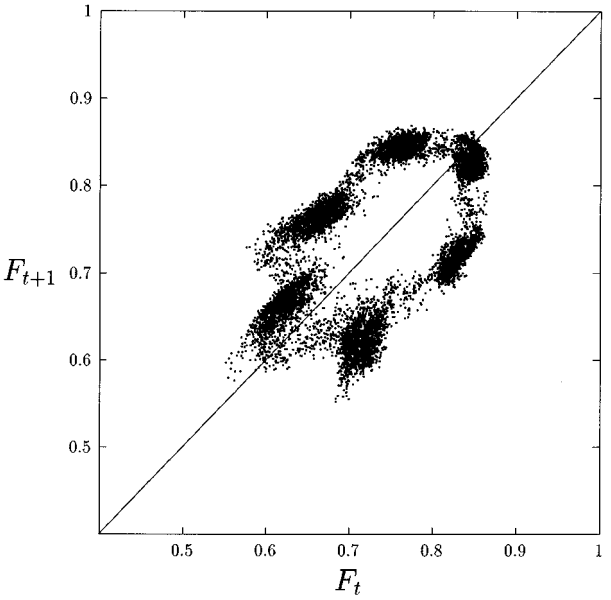

FIG. 2. Return map F_{t+1} vs F_t of the instantaneous turbulent fraction obtained from direct simulation of the globally coupled Chaté-Manneville maps. The parameters are $r=3$, $\epsilon=0.295$; and the system size is $N=10^5$. The number of iterations shown is 10^4.

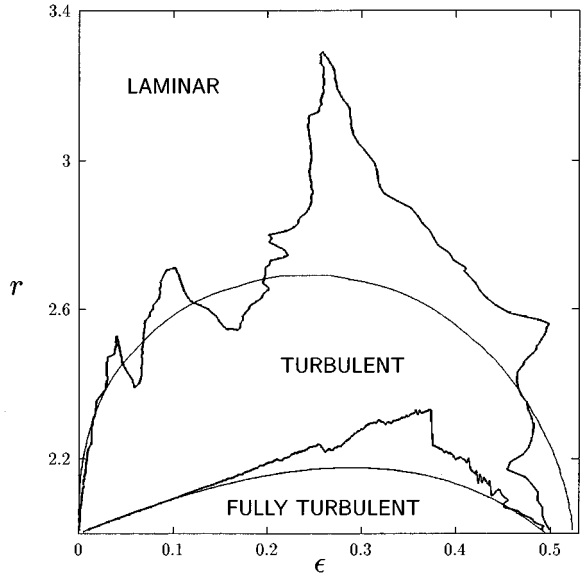

FIG. 3. Phase diagram of the globally coupled map system. The different stationary regimes of the system are indicated on the parameter plane. The numerically determined critical boundaries between laminar and turbulent states and between turbulent and fully turbulent regimes are shown with a thick line. The smooth (thin) curves correspond to the theoretical prediction of those same boundaries; upper curve: theoretical laminar-turbulent boundary, lower curve: theoretical turbulent fully turbulent boundary (Sec. III).

sibility of supporting small spatial domains of turbulent cells which would be necessary for a continuous transition to turbulence.

The error bars shown on the mean turbulent fraction $\langle F\rangle$ in Figs. 1(a) and 1(b) correspond to the standard deviation (square root of the variance) of the time series of F_t at each value of ϵ. With increasing system size N, these fluctuations turn out to decrease only up to some size, beyond which they remain constant. This phenomenon is associated to a nontrivial collective behavior commonly observed in globally coupled maps and which has been called ''violation of the law of large numbers'' [16]: the variance of the temporal fluctuations of the mean field [Eq. (2)] does not scale as N^{-1} for large N, but it saturates at some constant value. In the present case, the large amplitudes of the standard deviations observed in Fig. 1 reflect collective periodic states of the system. For example, Fig. 2 shows the return map of the instantaneous turbulent fraction F_{t+1} vs F_t for parameter values $r=3$ and $\epsilon=0.295$, after discarding the transients. The instantaneous turbulent fraction displays an approximate periodic behavior, with period *six*. Other nontrivial collective states can be observed at different parameter values of the system. The instantaneous turbulent fraction is a simpler statistical description than the mean field and, in our case, it already manifests a collective periodic behavior of the system over long times, as shown in Fig. 2. Calculations of return maps of the mean field of the system at parameter values giving turbulence should reveal more details on the nature of those collective behaviors, such as global periodic attractors and possible quasiperiodic motions.

We have calculated numerically the critical values ϵ_c, ϵ_c' corresponding to boundaries of the windows of turbulence observed in the system as a function of r. There exists a maximum value $r_{\max}\simeq 3.29$ beyond which no turbulent regime is observed. In this case, the coupling cannot compensate the escape rate from the interval $[0,1]$ in the local maps. Both parameters r and ϵ were varied in 10^{-3} in order to detect the regions of turbulence. Figure 3 shows the complex critical boundary for the onset of turbulence determined in this way. The structure of the turbulent windows in parameter space is revealed in Fig. 3. The fine structure of this critical boundary is actually more complex; there are several narrow windows of turbulence and laminar gaps at smaller scales. Some of the complexity of the critical boundary between turbulent and laminar regimes has already been suggested by less detailed calculations on diffusively coupled one-dimensional lattices [5,6]. For parameter values inside the critical boundary, the globally coupled map system exhibits sustained turbulence ($0<\langle F\rangle\leqslant 1$). The region where full turbulence takes place ($\langle F\rangle=1$) is also shown in Fig. 3. In this fully turbulent region, the globally coupled system, Eq. (1), uses only the regime $x\in[0,1]$ of the local map, Eq. (3). Thus the local dynamics is effectively a tent map with slope $r>2$. The global coupling is capable of confining all the elements $x_t(i)$ to the interval $[0,1]$, even though the local dynamics is repelling in this case. As found by Kaneko [17], a system of globally coupled tent maps with $r<2$ presents collective behaviors (one- and two-band global attractors) and a turbulent phase on different regions of its parameter plane (r,ϵ). One may expect that a simple extrapolation of the phase diagram in [17] should carry through this structure to the range $r>2$, corresponding to the fully turbulent region in Fig. 3. The laminar regime of the system ($\langle F\rangle=0$) occurs for values (r,ϵ) outside the critical boundary. This boundary signals the discontinuous transition between the two collec-

tive states (laminar and turbulent) in the phase diagram of the system. Figure 3 also shows a theoretical critical boundary for the onset of turbulence in globally coupled maps as well as a predicted boundary for full turbulence, both obtained from a model presented in the next section.

III. MAP FOR THE TURBULENT FRACTION

The existence of two distinct states (laminar and turbulent) in the local dynamics and the global coupling are simplifying features that permit the construction of a map for the instantaneous turbulent fraction in the system under consideration. In this case, it is possible to estimate the instantaneous exchange of cell values between the two states in order to compute the change of the F_t in one iteration.

Let ϕ_t^+ (ϕ_t^-) be the fraction of cells that being laminar (turbulent) at time t will become turbulent (laminar) at time $t+1$. Then, the change in the instantaneous turbulent fraction from one iteration to the next is

$$\Delta F_t \equiv F_{t+1} - F_t = \phi_t^+ - \phi_t^- . \tag{5}$$

A cell i that is laminar at time t becomes turbulent at time $t+1$ if

$$(1-\epsilon)x_t(i) + \epsilon h_t < 1; \tag{6}$$

therefore, ϕ_t^+ is the fraction of cells satisfying the condition $1 \leqslant x_t(i) < x_m$, where

$$x_m = \frac{1-\epsilon h_t}{1-\epsilon}. \tag{7}$$

The quantity x_m is the maximum value that laminar cells may have in order to become turbulent in the next iteration. Thus the fraction of the laminar range $[1, r/2]$ occupied by cells making the transition to turbulence in the next iteration is $(x_m - 1)/(r/2-1)$. Notice that

$$\phi_t^+ = 1 \quad \text{if} \quad x_m > r/2,$$
$$\phi_t^+ = 0 \quad \text{if} \quad x_m < 1. \tag{8}$$

For $x_m \in (1, r/2)$, we approximate the function ϕ_t^+ as

$$\phi_t^+ = (1-F_t)\left(\frac{x_m - 1}{r/2-1}\right)^{k_1}, \tag{9}$$

where the positive exponent k_1 is a parameter introduced to take into account the nonhomogeneous distribution of cells in the interval $[1, r/2]$.

Similarly, a cell i with $x_t(i) \leqslant 1/2$ becomes laminar in the next iteration if

$$(1-\epsilon) r x_t(i) + \epsilon h_t > 1, \tag{10}$$

while the same transition for a cell with $1/2 < x_t(i) < 1$ occurs if

$$(1-\epsilon)[1 - x_t(i)]r + \epsilon h_t > 1; \tag{11}$$

therefore, ϕ_t^- corresponds to the fraction of cells satisfying the condition $x_m/r < x_t(i) < 1 - x_m/r$. Notice that

$$\phi_t^- = 0 \quad \text{if} \quad x_m > r/2. \tag{12}$$

For $x_m < r/2$, we assume the following form of the function ϕ_t^-,

$$\phi_t^- = F_t\left(1 - 2\frac{x_m}{r}\right)^{k_2}, \tag{13}$$

where the quantity $(1 - 2x_m/r)$ is the fraction of the turbulent range $[0,1]$ occupied by cells that become laminar in the next iteration. The positive exponent k_2 takes into account the nonhomogeneous distribution of cells in the interval $[0,1]$.

By using the above assumptions, the difference map Eq. (5) can be written as

$$\Delta F_t = \begin{cases} -F_t\left(1 - \dfrac{2x_m}{r}\right)^{k_2} & \text{if } x_m \leqslant 1 \\ (1-F_t)\left(\dfrac{x_m - 1}{r/2-1}\right)^{k_1} - F_t\left(1 - \dfrac{2x_m}{r}\right)^{k_2} & \text{if } 1 < x_m < r/2 \\ 1 - F_t \quad \text{if } x_m \geqslant r/2. \end{cases} \tag{14}$$

The case $x_m \leqslant 1$ (i.e., $\phi_t^+ = 0$) describes transient turbulent regimes evolving towards a final laminar state ($F_t = 0$). In the case $x_m \geqslant r/2$ (i.e., $\phi_t^- = 0$ and $\phi_t^+ = 1$), the system reaches a fully turbulent regime ($F_t = 1$) in one time step.

To obtain the explicit dependence of the difference map Eq. (14) on the parameters r and ϵ, we need an expression for h_t. The instantaneous mean-field h_t can be approximated as the sum of two contributions

$$h_t = h_T(r,\epsilon)F_t + h_L(r,\epsilon)(1-F_t), \tag{15}$$

where h_T and h_L are the instantaneous mean fields of the turbulent and of the laminar cells, respectively. In particular, the instantaneous mean-field h_T of the turbulent cells fluctuates for fixed values of r and ϵ. When h_T approaches the value 1, the system tends to fall to the laminar state; thus the maximum values of h_T in parameter space are the relevant ones for the transition to turbulence. From the numerical calculations, one can roughly approximate h_T and h_L as

$$h_T \simeq 0.48 + 1.05\epsilon, \tag{16}$$

$$h_L \simeq 1 + 0.10(r-2). \tag{17}$$

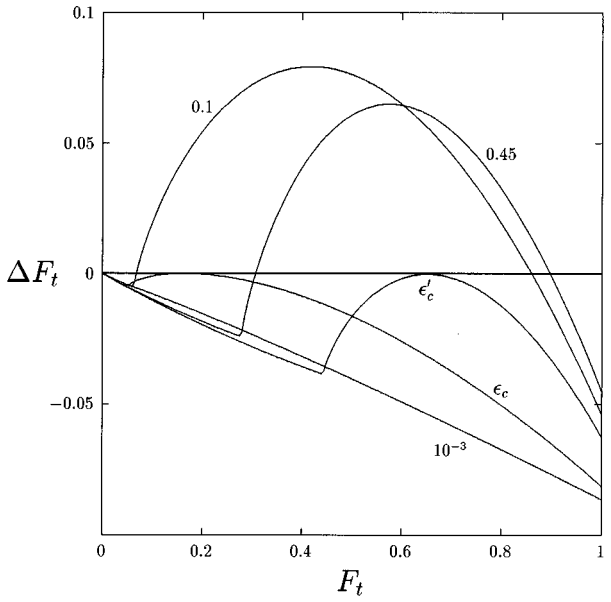

FIG. 4. The map ΔF_t vs F_t obtained from Eq. (14) plotted for five labeled values of ϵ and fixed value $r=2.3$. The critical values for the onset of turbulence are $\epsilon_c=0.0145$ and $\epsilon_c'=0.488$.

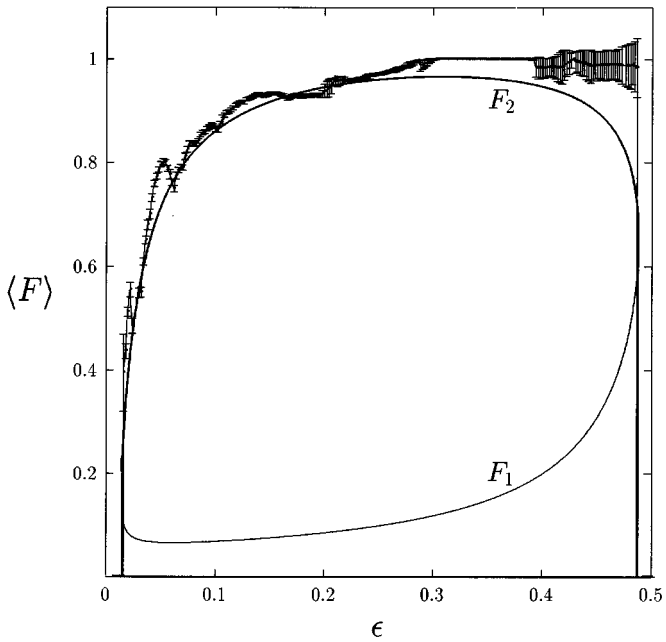

FIG. 5. Numerically calculated mean turbulent fraction $\langle F \rangle$ as a function of the coupling ϵ for fixed $r=2.3$. The system becomes fully turbulent ($\langle F \rangle=1$) between $\epsilon\simeq 0.31$ and $\epsilon\simeq 0.39$. The error bars indicate ± 1 standard deviations. The stable fixed point F_2 (thick line) and the unstable fixed point F_1 (thin line) of the map Eq. (14) are also shown as functions of ϵ for $r=2.3$.

The expression for h_T reflects the fact that the range of allowed values in the turbulent phase does not depend on r, while an increase of the coupling ϵ enhances the flow of laminar cells across the phase boundary $x=1$, producing an increment of the population of turbulent cells with $x(i)>1/2$. On the other hand, since the range of allowed values in the laminar phase is $(r/2-1)$, one could expect h_L to increase with r. The above approximations are sufficient for the construction of a mapping of the turbulent fraction, Eq. (14), that describes many relevant properties of the globally coupled Chaté-Manneville maps.

Figure 4 shows ΔF_t vs F_t obtained from Eq. (14) for five different values of ϵ and the fixed value $r=2.3$. The exponents $k_1=0.8$ and $k_2=1.2$ were chosen in all the calculations since they optimize the agreement of our model with the results from the globally coupled map system, but the characteristics of the map model persist for a range of values of the parameters k_1 and k_2. The real roots ($\Delta F_t=0$) of Eq. (14) give the fixed points (stationary values) of the turbulent fraction F_t. The laminar state $F_t=0$ is always a stable fixed point. Additionally, two other fixed points, F_1 and F_2 ($F_1<F_2$), occur in the interval $\epsilon\in[\epsilon_c,\epsilon_c']$, as shown in Fig. 4. The fixed point F_1 is unstable and it defines a critical value of the instantaneous turbulent fraction bellow which the system invariably falls to the the stable laminar state $F_t=0$. For values of the instantaneous turbulent fraction above this critical value F_1, the system evolves towards the upper fixed point F_2, which is stable. As shown in Fig. 4 and in Fig. 5, the two nonvanishing fixed points coincide at the critical values of the coupling ϵ_c and ϵ_c' corresponding to tangent bifurcations of the map Eq. (14). In Fig. 5 the fixed points of the map Eq. (14) are plotted as a function of ϵ, for fixed $r=2.3$. Figure 5 clearly shows that at the critical values of the coupling ϵ_c and ϵ_c' the transition between laminar ($F_t=0$) and turbulent ($F_t=F_2$) regimes predicted by the map Eq. (14) is discontinuous, as seen in the numerical calculations. The mean turbulent fraction $\langle F \rangle$ obtained from direct simulations of the globally coupled map system with $r=2.3$ is also shown as a function of ϵ in Fig. 5. The stable fixed point F_2 obtained from the map model agrees well with the direct calculation.

The values ϵ_c and ϵ_c' corresponding to each value of r define the boundary between laminar and turbulent regimes in the parameter space. The curves $\epsilon_c(r)$ and $\epsilon_c'(r)$ obtained from the model are shown in Fig. 2. By comparing with the critical boundary resulting from direct calculations, one can see that the model given by Eq. (14) provides a qualitative description of the transition to turbulence in the globally coupled map system. For values of r close to 2 and small ϵ, the model reproduces quite well the critical boundary. The map model also predicts the existence of a boundary for the fully turbulent region in the parameter plane. On this boundary, $x_m=r/2$ and $h_t=h_T$; thus from Eq. (7), we get

$$r\simeq\frac{2}{1-\epsilon}[1-\epsilon(0.48+1.05\epsilon)]. \tag{18}$$

This curve is also plotted in Fig. 2. However the simple model presented here fails to reproduce the complex structure of the critical boundary and it predicts a lower value for the maximum value of r for which turbulence can be sustained.

IV. CONCLUSIONS

Some of the features associated with the occurrence of turbulence in globally coupled systems have been explored in this paper. We have found that the onset of turbulence

occurs discontinuously at critical values of the parameters, as in first order phase transitions. Previous studies of diffusively coupled map lattices with Chaté-Manneville local dynamics have shown that the transition to turbulence in those cases is similar to a second order phase transition.

We have made detailed calculations that reveal the complexity of the critical boundaries separating the different regimes of the system. Multiple windows of turbulence and relaminarization of the system have been observed as the coupling parameter is varied.

Nontrivial collective behavior arises within the turbulent region in the parameter space of the globally coupled system. In fact, the return map of the instantaneous fraction of turbulent cells, which is a simple two-state statistical description of the system, reflects this collective temporal organization. The appearance of nontrivial collective behaviors in map lattices with local or global couplings is a subject of current research. Much effort has been devoted to establishing the necessary conditions for the emergence of this behavior. Periodic collective states have been found in globally coupled maps belonging to some universality class (tent, quadratic, or circle maps) [17,18]. The observation of collective periodic behavior in the present system, where the local dynamics has very specific characteristics, suggests that this kind of collective behavior should be a rather common phenomenon in deterministic systems of coupled chaotic elements.

The proposed map for the instantaneous turbulent fraction explains many of the observed aspects of the globally coupled Chaté-Manneville maps, such as: the existence of the critical values of the coupling ϵ_c and ϵ_c' and the critical boundary in parameter space for the transition to turbulence; the discontinuos character of the transition; the existence of an $r_{\max}$; the presence of a threshold for the initial turbulent fraction in order to develop sustained turbulence; and the existence of a fully turbulent regime and its boundary in the parameter plane.

The global map cannot describe the complex structure of the critical boundary and it predicts a lower value of $r_{\max}$. The theoretical critical boundary becomes less accurate, with respect to the direct simulations, for large values of r and ϵ. However, map models for global quantities, such as the mean field or other statistical properties of the system, constitute an useful approach for the understanding of the collective dynamics of coupled map lattices. In particular, global maps analogous to Eq. (14) could model the behavior of other globally coupled systems whose local dynamics contains two distinct states, as in bistable maps.

ACKNOWLEDGMENTS

This work was supported by Grant Nos. C-717-95 and C-658-94 from the Consejo de Desarrollo Científico, Humanístico y Tecnológico of Universidad de Los Andes, Venezuela. We thank the International Center for Theoretical Physics at Trieste for the hospitality while part of this work was carried out.

[1] See, for example, A. C. Newell, in *Perspectives in Nonlinear Dynamics*, edited by M. F. Shlesinger *et al.* (World Scientific, Singapore, 1986); J. Crutchfield and K. Kaneko, in *Directions in Chaos I*, edited by H. Bai-Lin (World Scientific, Singapore, 1987); P. Manneville, *Dissipative Structures and Weak Turbulence* (Academic, Boston, 1990).
[2] K. Kaneko, Prog. Theor. Phys. **74**, 1033 (1985).
[3] S. Ciliberto and P. Bigazzi, Phys. Rev. Lett. **60**, 286 (1988).
[4] H. Chaté and P. Manneville, Physica D **32**, 409 (1988); Europhys. Lett. **6**, 591 (1988).
[5] J. Houlrik, I. Webman, and M. H. Jensen, Phys. Rev. A **41**, 4210 (1990).
[6] J. R. de Bruyn and L. Pan, Phys. Rev. E **47**, 4575 (1993).
[7] P. Grassberger and T. Schreiber, Physica D **50**, 177 (1991).
[8] M. G. Cosenza and R. Kapral, Chaos **4**, 99 (1994).
[9] H. Chaté and P. Manneville, Phys. Rev. Lett. **58**, 112 (1987).
[10] P. Hadley and K. Wiesenfeld, Phys. Rev. Lett. **62**, 1335 (1989).
[11] K. Wiesenfeld, C. Bracikowski, G. James, and R. Roy, Phys. Rev. Lett. **65**, 1749 (1990).
[12] S. H. Strogatz, C. M. Marcus, R. M. Westervelt, and R. E. Mirollo, Physica D **36**, 23 (1989).
[13] N. Nakagawa and Y. Kuramoto, Physica D **75**, 74 (1994).
[14] K. Kaneko, Physica D **75**, 55 (1994); **77**, 456 (1994).
[15] K. Kaneko, Physica D **41**, 137 (1990).
[16] K. Kaneko, Phys. Rev. Lett. **65**, 1391 (1990).
[17] K. Kaneko, Physica D **55**, 368 (1992).
[18] K. Kaneko, Physica D **86**, 158 (1995).